# Supplemental Information

## Dynamic RNA binding and unfolding by nonsense-mediated mRNA decay factor UPF2

**Authors:**

Jenn-Yeu A. Szeto [1†], Mirella Vivoli Vega [1†], Justine Mailliot [1], George Orriss [1], Lingling Sun [1], Joshua C. Bufton [1], Kyle T. Powers[1], Sathish K.N. Yadav [1], Imre Berger [1,2,3] and Christiane Schaffitzel [1*]

**Affiliations:**

[1] School of Biochemistry, University of Bristol; University Walk, Bristol, BS8 1TD, UK

[2] School of Chemistry, University of Bristol, Cantock's Close, Bristol BS8 1TS, UK.

[3] Max Planck Bristol Centre for Minimal Biology, Cantock's Close, Bristol BS8 1TS, UK

[†] These authors contributed equally to this work.

* Correspondence to: christiane.berger-schaffitzel@bristol.ac.uk

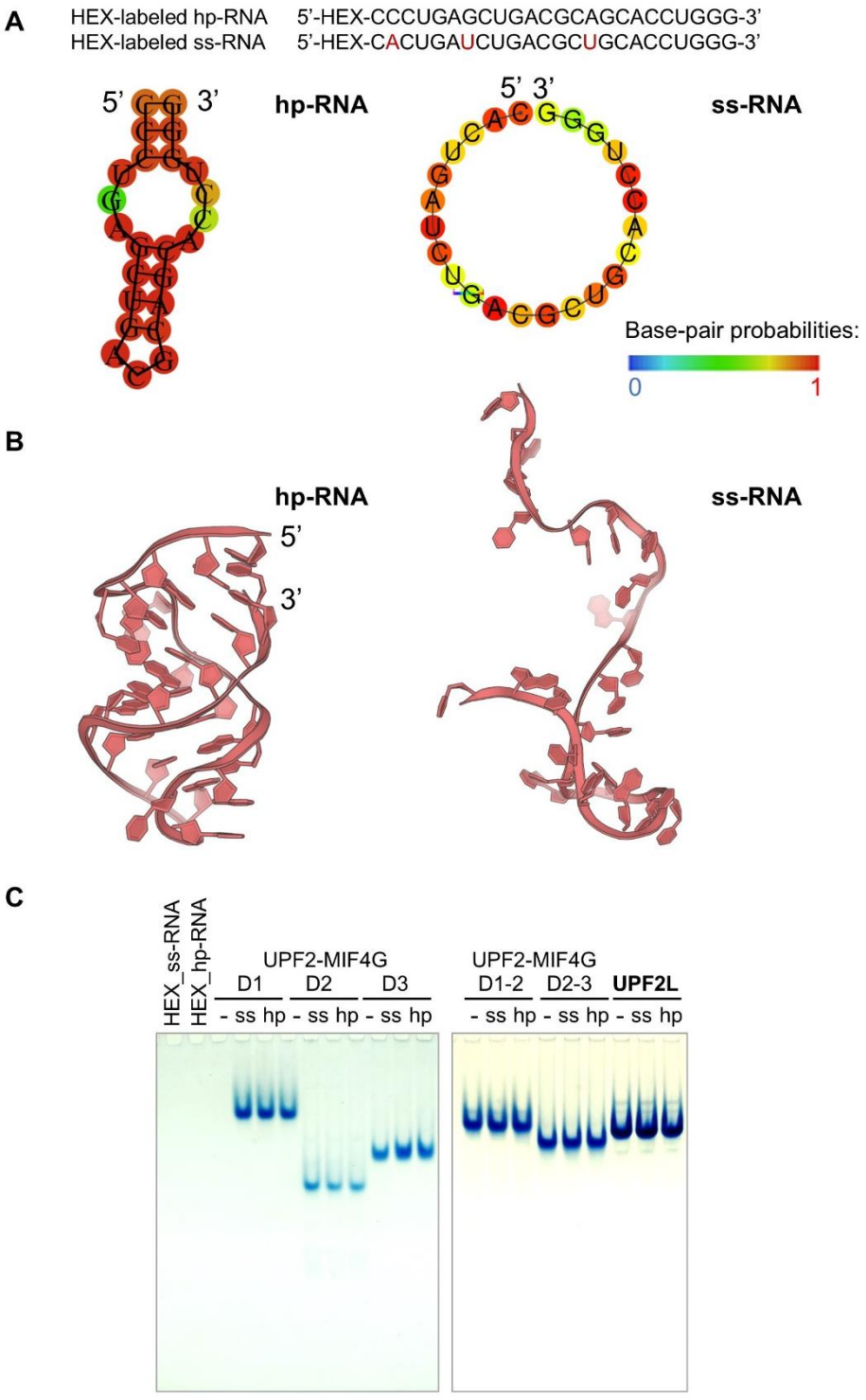


**Supplemental Figure S1: RNA binding of UPF2 variants tested by EMSAs. (A)** Sequence and structure of hexachlorofluorescein (HEX)-labeled RNA constructs used for EMSAs. RNA secondary structure prediction through energy minimization RNAfold (Lorenz et al. 2011). **(B)** 3D models of hp-RNA and ss-RNA predicted using 3dRNA/DNA (Zhang et al. 2022) and trRosettaRNA (Wang et al. 2023) leading to virtually identical predictions. **(C)** Coomassie-stained EMSA gels showing the UPF2 protein constructs from Figure 1F. A shift in protein towards higher molecular weight upon RNA binding is not observed.

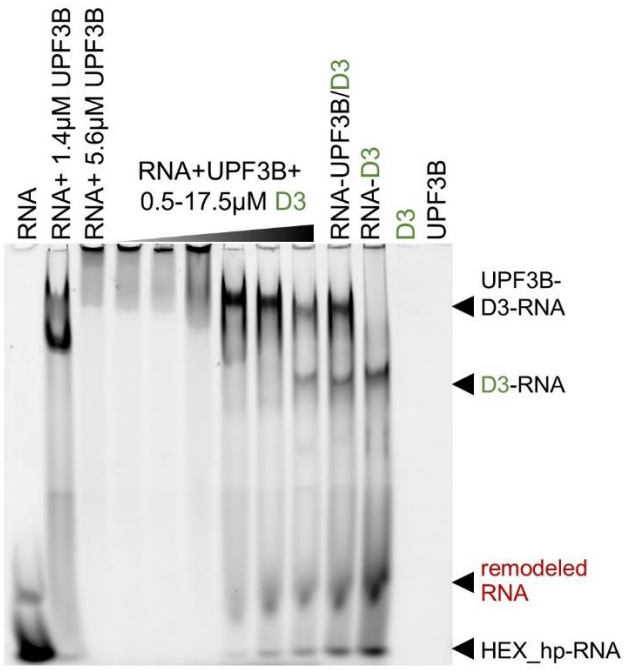


**Supplemental Figure S2: MIF4G-D3 RNA binding in the presence of UPF3B.** EMSA gel with 250 nM HEX_hp-RNA in all lanes, except the MIF4G-D3 only and the UPF3B only controls. As controls, HEX_hp-RNA was loaded alone or mixed with 1.4 μM UPF3B indicative of a 1:1 molar complex. HEX_hp-RNA premixed with 5.6 μM UPF3B exhibits RNA-induced oligomerization, to which increasing concentrations of UPF2 MIF4G-D3 was added. At approximately 1:1 molar ratio of UPF3B and MIF4G-D3, a stoichiometric complex with RNA is observed, together with the appearance of a remodeled RNA band (highlighted in red).

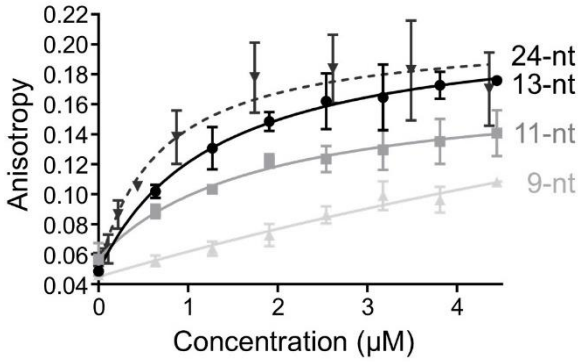


| Construct | ss-RNA | $K_D$ (nM) |
|---|---|---|
| MIF4G-D3 | HEX_24-nt | 694±189 |
| MIF4G-D3 | HEX_13-nt (PUR) | 1,281±297 |
| MIF4G-D3 | HEX_11-nt (PUR) | 1,774±628 |
| MIF4G-D3 | HEX_9-nt (PUR) | (17,500±14,000) |

**Supplemental Figure S3: Nucleic acid-binding of UPF2 MIF4G-D3 tested by fluorescence anisotropy.** Fluorescence anisotropy binding curves of UPF2 MIF4G-D3 to HEX-labeled purine-rich (PUR) ss-RNA of varying lengths (left). Measurements were performed in triplicate and error bars plotted via standard deviation before fitting a single component binding equation to calculate $K_D$ values (right). The $K_D$ value for binding the 9-nt oligomer is an estimate. Sequences are listed in Supplemental Table S1.

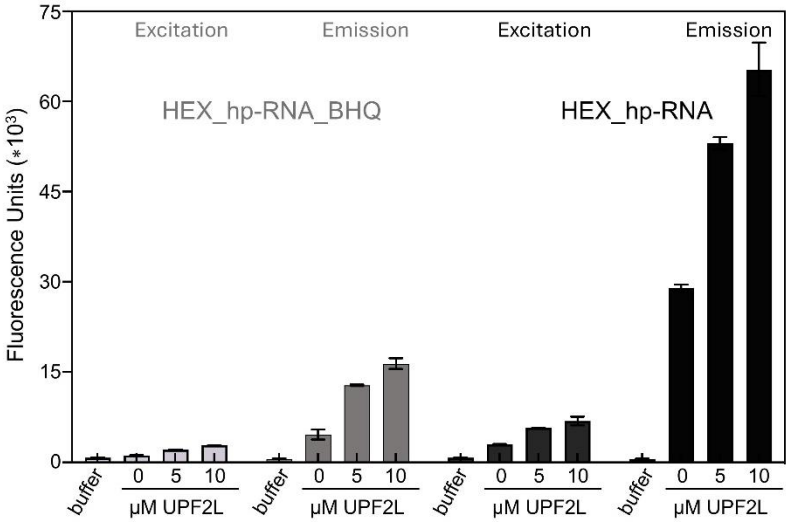


**Supplemental Figure S4: RNA structural changes mediated by UPF2L.** Changes of the relative excitation and emission intensities, respectively, of hexachlorofluorescein (HEX) fluorophore were monitored at 539 nm and 559 nm respectively. HEX-labeled hp-RNAs with blackhole quencher 1 (HEX_hp-RNA_BHQ, grey bars) or without BHQ (HEX_hp-RNA, black bars) were assayed in the presence of different concentrations of UPF2L and compared to buffer only (first bar of each series). Experiments were performed in duplicate. Standard deviations are shown as bars.

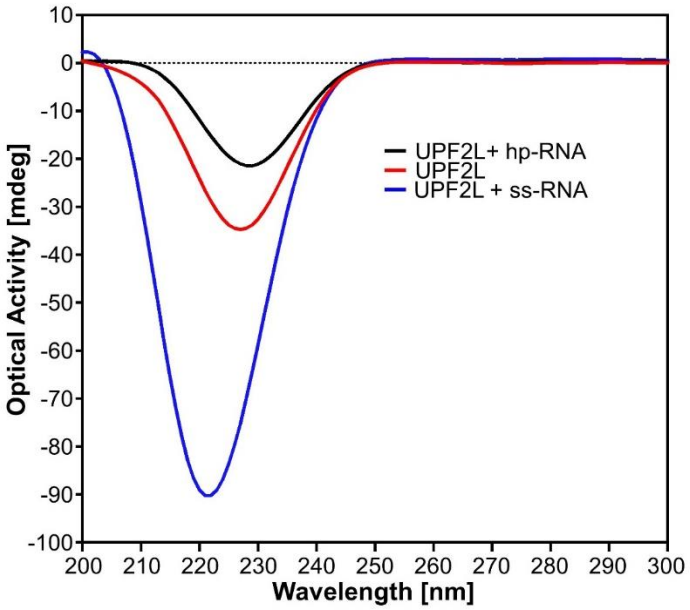


**Supplemental Figure S5: CD spectroscopy of UPF2L and UPF2L in complex with hp-RNA or ss-RNA.** CD spectra of UPF2L (red) and of UPF2L in the presence of ss-RNA (blue) or the presence of hp-RNA (black), respectively. The UPF2L + hp-RNA complex curve presents the difference between the curve of the UPF2L/ hp-RNA complex and the curve of hp-RNA alone. The UPF2L + ss-RNA complex curve presents the difference between the curve of the UPF2L/ ss-RNA complex and the curve of ss-RNA alone. Experiments were performed in duplicate.

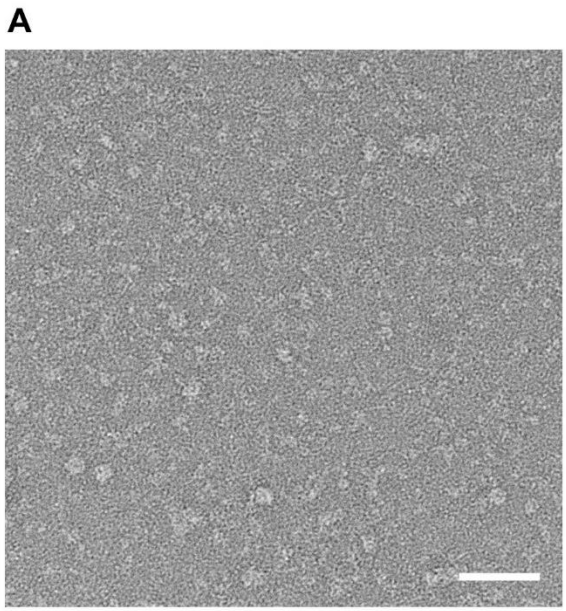


| Sample | No. of Particles | Elongated Shape | Compact Shape |
|---|---|---|---|
| UPF2L | 71,643 | 64,948 (90%) | 7,145 (10%) |
| UPFL + hp-RNA | 71,724 | 38,013 (53%) | 33,711 (47%) |
| UPF2L + ss-RNA | 154,197 | 11,894 (8%) | 142,303 (92%) |

**Supplemental Figure S6: Negative-stain EM of UPF2L alone and in complex with hp-RNA or ss-RNA, respectively. (A)** Micrograph of UPF2L alone. **(B)** Micrograph of UPF2L incubated with 4-fold molar excess of hp-RNA. **(C)** Micrograph of UPF2L incubated with ss-RNA in a 1:4 molar ratio. **(A-C)** Scale bar: 50 nm. **(D)** Table listing the number of particles picked from negative-stain EM micrographs for the three samples, the number of particles with an elongated shape and the number of particles with a compact conformation (the percentages are indicated in brackets).

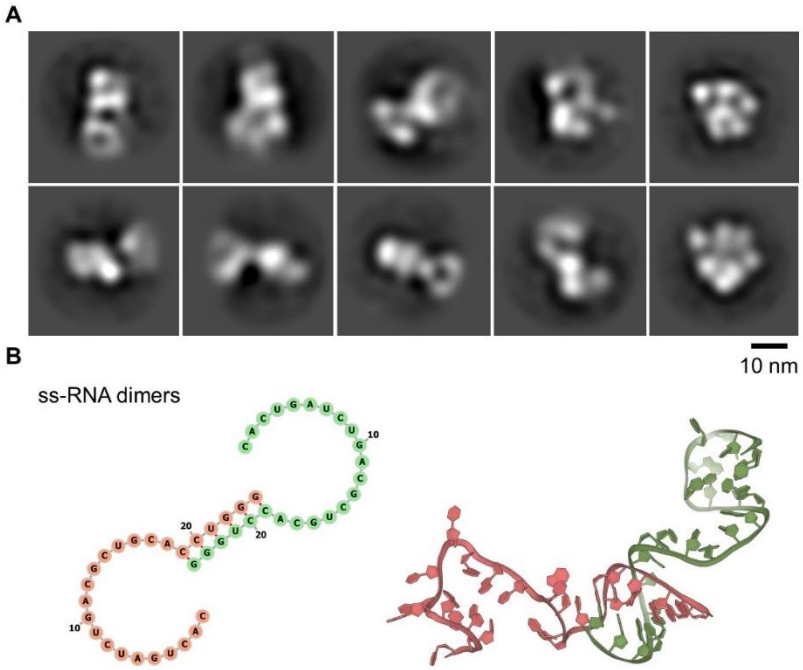


**Supplemental Figure S7: UPF2L dimers observed in the presence of 24-nt ss-RNA (A)** 2D class averages of UPF2L incubated with ss-RNA showing dimers. **(B)** To predict potential 2D and 3D RNA dimer models, a $U_{10}$ or $A_{10}$ linker (not shown) was inserted between the two ss-RNA sequences. 2D and 3D models of ss-RNA dimers are shown, predicted using MXfold2 (Sato et al. 2021) and 3dRNA/DNA (Zhang et al. 2022). trRosettaRNA (Wang et al. 2023) does not predict dimerization of the ss-RNA.

**Supplemental Table S1.** Sequences of the hexachlorofluorescein (HEX)-labeled RNA and DNA constructs used for fluorescence anisotropy measurements and EMSAs.

| **Oligonucleotide name** | **Sequence** |
|---|---|
| HEX_hp-RNA (24-nt) | 5'-HEX-CCCUGAGCUGACGCAGCACCUGGG |
| **Single-stranded RNA constructs** | |
| HEX_ss-RNA (24-nt) | 5'-HEX-CACUGAUCUGACGCUGCACCUGGG |
| HEX_PUR-ss-RNA (13-nt) | 5'-HEX-AAAUGAAGAUAAA |
| HEX_PUR-ss-RNA (11-nt) | 5'-HEX-AAUGAAGAUAA |
| HEX_PUR-ss-RNA (9-nt) | 5'-HEX-AUGAAGAUA |
| HEX_PYR-ss-RNA (13-nt) | 5'-HEX-UUUACUUCUAUUU |
| HEX_PYR-ss-RNA (11-nt) | 5'-HEX-UUACUUCUAUU |
| **Double-stranded RNA construct** | |
| HEX_ds-RNA (24-nt) | 5'-HEX-CCCUGAGCUGACGCAGCACCUGGG<br>GGGACUCGACUGCGUCGUGGACCC-5' |
| **Single-stranded DNA construct** | |
| HEX_ss-DNA (24-nt) | 5'-HEX-CCCTGAGCTGACGCAGCACCTGGG |
| **Double-stranded DNA construct** | |
| HEX_ds-DNA (24-nt) | 5'-HEX-CCCTGAGCTGACGCAGCACCTGGG<br>GGGACTCGACTGCGTCGTGGACCC-5' |